

## Time Variability of Galactic CRs and the Diffuse TeV Gamma-Ray Emission Predicted with GALPROP

P. D. Marinos,<sup>a,\*</sup> G. P. Rowell,<sup>a</sup> T. A. Porter<sup>b</sup> and G. Jóhannesson<sup>c</sup>

<sup>a</sup>*School of Physical Sciences, University of Adelaide,  
Adelaide, South Australia 5000, Australia*

<sup>b</sup>*W. W. Hansen Experimental Physics Laboratory and Kavli Institute for Particle Astrophysics and  
Cosmology, Stanford University,  
Stanford, CA 94305, USA*

<sup>c</sup>*Science Institute, University of Iceland,  
IS-107 Reykjavik, Iceland*

*E-mail:* [peter.marinosa@adelaide.edu.au](mailto:peter.marinosa@adelaide.edu.au), [gavin.rowell@adelaide.edu.au](mailto:gavin.rowell@adelaide.edu.au),  
[tporter@stanford.edu](mailto:tporter@stanford.edu), [gudlaugu@hi.is](mailto:gudlaugu@hi.is)

Using the 3D simulation software GALPROP, we modelled the Galactic cosmic ray (CR) diffusion and investigated the time variability of the gamma-ray flux along the Galactic plane using a distribution of stochastically placed CR sources. These CR sources more accurately represent the formation rate and finite lifetimes compared to the steady-state CR injection models that are typically assumed. Our results show that the leptonic component of the gamma-ray emission is highly sensitive to the assumed electron injection and spectral characteristics. Furthermore, the leptonic component is heavily dependent on the positions of the sources due to the rapid synchrotron cooling of the very-high-energy electrons. At 1 TeV the total gamma-ray flux along the Galactic plane can vary by as much as 50% due only to the stochasticity of the CR source placement. The large-scale gamma-ray emission that CTA will observe will be significantly influenced by gamma rays local to CR accelerators. The variability in the modelled large-scale gamma-ray emission will have important implications for any background modelling that CTA (or any other TeV observatory) performs. Hence, we will also provide the first look at the time-dependent morphology in the multi-TeV gamma-ray structures in the Milky Way and quantify the variation over time and Galactic longitude.

38th International Cosmic Ray Conference (ICRC2023)  
26 July - 3 August, 2023  
Nagoya, Japan



---

\*Speaker

## 1. Introduction

Cosmic ray (CR) particles are accelerated up to PeV energies and can diffuse through the Milky Way (MW) for millions of years, resulting in a diffuse ‘sea’ of CRs. The CRs lose energy and emit non-thermal broad-band emissions due to interactions with the various components of the interstellar Medium (ISM); the interstellar gas, the interstellar radiation field (ISRF), and the Galactic magnetic field (GMF). Observations of these emissions are essential to understanding how the CRs are accelerated up to these energies and for understanding how they travel through the MW. Observations of  $\gamma$  rays can also constrain the spatial distributions of the ISM components.

The standard procedure for Galactic diffusion calculations is to inject CRs based on a smoothly-varying source distribution. In reality, CRs are injected into the ISM by individual sources with finite lifetimes. The observed diffuse CR sea is then created from the ensemble of all CR accelerators. Due to the CR spectra softening as the CRs diffuse away from their sources, and as the Galactic CR sources exist for some finite length of time, there will be some energy where the fluctuations due to individual sources will outshine the diffuse flux of CRs. The magnitude of the temporal variations will depend on the distribution of the CR sources, the injection spectra of the CR sources, the creation rate of the CR sources, and the lifetimes of the CR sources.

Temporal variation in the CRs will necessarily impart a component of temporal variation onto the  $\gamma$ -ray sky. Accurately modelling CR propagation and the local CR fluxes would require precise position and spectral information on all CR accelerators in the MW within  $\sim 1$  kpc of the Solar location. Accurately modelling the VHE  $\gamma$ -ray sky would require precise positional and spectral information beyond  $\sim 1$  kpc. As this data is not currently known, any temporal variation that arises from randomly placing CR sources is an additional modelling uncertainty that remains to be quantified. This uncertainty impacts all CR propagation codes and their VHE  $\gamma$ -ray emission predictions.

Previous results from [1] found that for  $\gamma$ -ray energies above 1 TeV the electron IC emissions had an increasing contribution to the total  $\gamma$ -ray flux observed along the Galactic plane. Additionally, features in the local CR electron flux will have a strong dependence on the proximity to nearby CR electron accelerators. Hence, for the CR electrons with energies  $>10$  TeV the placement of the individual sources has an impact on both local CR measurements as well as estimates of the  $>10$  TeV diffuse Galactic  $\gamma$ -ray emission.

In this contribution we use the time-dependent solution available in the GALPROP CR propagation package [2, 3] to quantify the variations in both the CR and  $\gamma$ -ray fluxes as a function of energy. We will quantify this uncertainty only for a single combination of ISM distributions; however, we do not expect the degree of uncertainty to change dramatically across the available range of reasonable models. We will also quantify the impacts that the temporal variability will have on future observations of the diffuse  $\gamma$ -ray emission such as, for example, by CTA.

## 2. Modelling Setup

The GALPROP framework [4, 5] is a widely employed CR propagation package that now has over 25 years of development behind it. For this paper, we use the latest release (v57), where an extensive description of the current features is given by [3].

## 2.1 Input Distributions

One of the critical inputs for a GALPROP run is the CR source distribution, i.e. the locations in the MW where the CRs are injected. Under the steady-state assumption the source distribution represents the relative amplitude of the injection spectra of CRs at a given location. In this work we use the time-dependent solution, which instead utilises the source distribution as a synthetic probability density function to stochastically place individual/discrete CR injection sites across the MW [2, 3]. The CR source distribution is defined as a sum of a disc-like component and a spiral-arm component. Here we use a source distribution that gives an equal weighting to the two components, such that half of the local CR flux comes from the disc and half from the spiral arms (termed SA50). For a description of the construction of the source distribution used here, see [1] and references therein.

The propagation and emissions of VHE CR electrons and positrons are largely controlled by the interstellar radiation field (ISRF) and the Galactic magnetic field (GMF). Furthermore, the pair-absorption effects on the  $>10$  TeV  $\gamma$  rays are completely regulated by the ISRF spatial and spectral distribution. Here we utilise the ‘R12’ ISRF model and the ‘PBSS’ GMF model (see [1], and references therein). Both of these models include the Galactic spiral arms. For the input ISM gas distribution, see [1, 6], and references therein.

## 2.2 Modelling Parameters

The critical condition is that the chosen combination of the inputs described above reproduces the local CR spectra. To ensure that the local spectra are reproduced, the propagation parameters and source spectra are optimised following [1]. We use the  $XY$  limits of  $\pm 20$  kpc and the  $Z$  limits of  $\pm 6$  kpc. We use the previous IAU recommended distance from the GC to the Solar location of  $R_s = 8.5$  kpc, such that it agrees with the other models used in the simulation. The Solar location in our coordinate system is given by  $(X, Y, Z) = (8.5, 0, 0)$  kpc. For runtime efficiency we use a non-linear grid (tan spatial grid). For the CRs, we use ten kinetic energy bins per decade ranging from 1 GeV/nuc to 10 PeV/nuc. For the  $\gamma$  rays, we use five energy bins per decade ranging from 1 GeV to 1 PeV. The  $\gamma$ -ray skymaps use a seventh-order HEALPix [7] isopixelisation, giving a pixel size of  $27.5'$ .

For the time-dependent solution we do not define the individual CR accelerator source types (e.g. SNRs, PWNe, stellar clusters, and binary sources). Currently, the relative CR contribution in the MW between the various source classes is not constrained adequately. Instead, we approximate some ‘average’ source, which is largely based on SNRs as they are believed to be the principal CR source class. The source parameters are tuned under the steady-state and diffuse assumptions, which injects CRs based on the smoothly-varying source distribution and does not model individual sites of injection. The CR spectra for the steady-state solution is then applied to each individual source in the time-dependent solution.

For the time-dependent solution, the rate and lifetime of the CR injection regions must also be considered. Similarly as for the above, instead of simulating impulsive and continuous sources separately we approximate the situation into a single source type. The source creation rate and the source lifetime are additional free parameters which do not impact the CR normalisation condition. However, the degree of variation will be impacted. There is no tight constraint on the estimates of the rates and lifetimes of the various classes of CR accelerator in the MW. For this work we

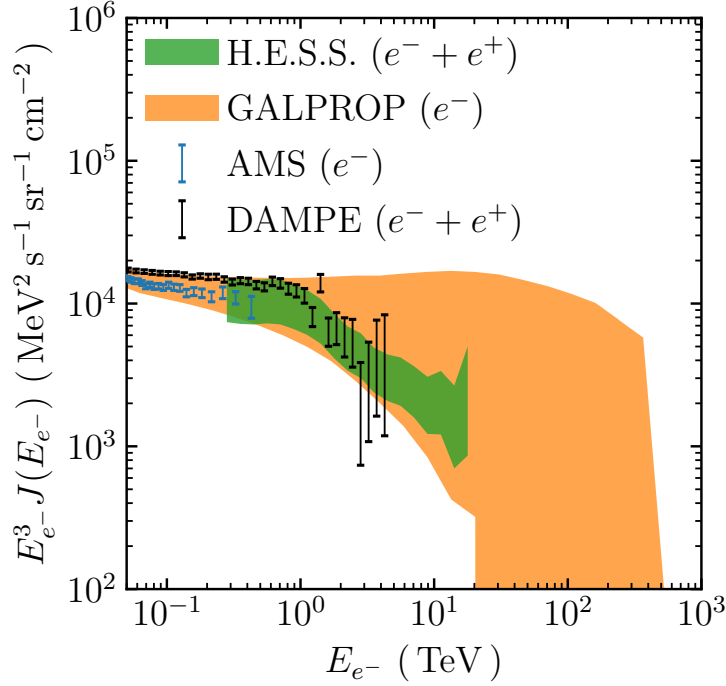


**Figure 1:** The variation in the simulated GALPROP electron kinetic energy spectrum above 50 GeV taken at the Solar location over a 5 Myr period is shown in orange. The preliminary H.E.S.S. combined electron and positron spectrum is from [8], the AMS electron spectrum is from [9], and the DAMPE combined electron and positron spectrum is from [10].

follow [2] and take a creation rate of one CR accelerator every 100 yr and a single source lifetime of 100 kyr.

We run the CR diffusion until the CR flux density across the entire MW has reached some steady state value. After this epoch, all variations in the CR and  $\gamma$ -ray flux will be due to the placement of the CR sources and centred around the steady-state flux values. The steady-state flux for the kinetic energy range of interest required 100 Myr of simulation time. CR diffusion calculations were then continued for an additional 5 Myr to obtain information on the variations around the steady-state fluxes. All results shown in this work use only the final 5 Myr of data for the analyses, with a 25 kyr step between outputs.

### 3. Results

Recent observations from DAMPE [10] and the preliminary results from H.E.S.S. [8] show a potential cut-off/break at  $\sim 1$  TeV for the combined electron and positron flux. Any TeV cut-off in the electron spectrum is explained naturally by the short ( $< 500$  pc) cooling distances of the VHE electrons – any measurement at the Solar location can only probe the local environment. Figure 1 shows the combined electron and positron flux DAMPE and H.E.S.S., as well as the electron flux from AMS [9]. An envelope of the variation in the local electron flux from GALPROP is shown for a 5 Myr period. The GALPROP electron flux shows a potential cut off at all timesteps, with the cut-off

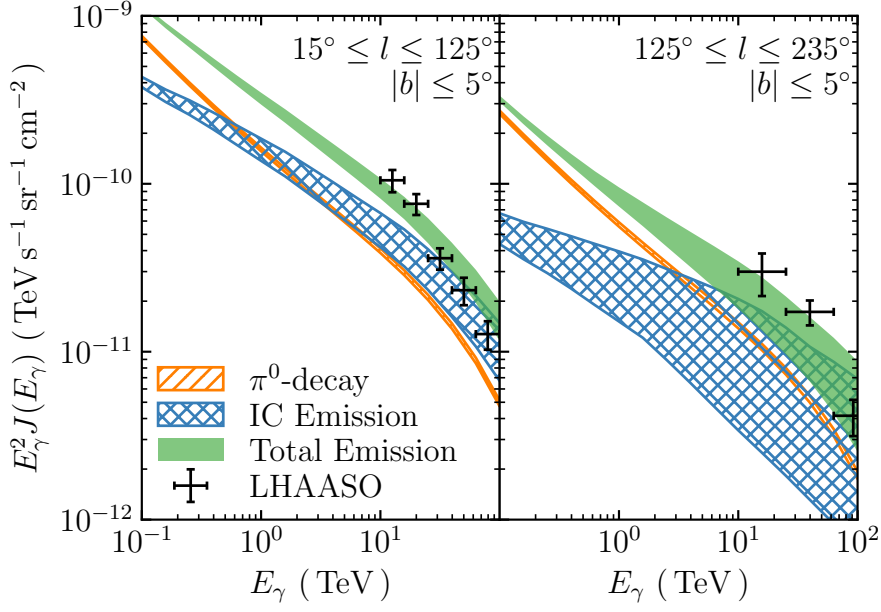


**Figure 2:** The variation in the simulated GALPROP  $\gamma$ -ray spectra for a 5 Myr period for the inner ( $15^\circ \leq l \leq 125^\circ$ ,  $|b| \leq 5^\circ$ ) and outer ( $125^\circ \leq l \leq 235^\circ$ ,  $|b| \leq 5^\circ$ ) LHAASO regions. The  $\pi^0$ -decay emission is shown by the orange hatched bands, the IC emission is shown by the blue hatched bands, and the total emission is shown by the green shaded region. The LHAASO flux points [11] are shown by the black points.

energy varying between  $\sim 800$  GeV and 60 TeV, depending on the proximity between Earth and the nearest electron accelerator at any given timestep. At 10 TeV the local electron flux varies by up to a factor of ten.

As the TeV protons (and heavier nuclei) travel distances  $> 1$  kpc there is little variation over time in the local hadronic spectra. The integration over the line-of-sight for the  $\gamma$ -ray calculations further reduces the variability in the hadronic  $\gamma$  rays. The  $\gamma$ -ray flux for two of the LHAASO regions is shown in Figure 2. For all Galactic longitudes, the pion-decay emission is constant over the 5 Myr simulation period. For the leptonic emission, the variability in the electrons is imparted onto the IC emissions. As the  $\gamma$ -ray energy increases, so does the variability of the IC emission. Furthermore, for the outer LHAASO region the line-of-sight integral contains less of the ISM, and so is more sensitive to variations in the electron density at any given location.

For  $\gamma$ -ray energies  $> 1$  TeV in the inner LHAASO region, and for  $> 10$  TeV for the outer LHAASO region, the IC emission can equal the pion-decay emission for some epochs. For the inner LHAASO region the IC emission dominates over the pion-decay for  $\gamma$ -ray energies above 10 TeV for all epochs in the simulation. The dominance of the IC emission for the inner Galaxy agrees with the results from [1]. Furthermore, the total  $\gamma$ -ray emission is within the uncertainties of the LHAASO diffuse flux estimates [11] for all timesteps in the simulation.

We applied a sliding window analysis to the GALPROP results, with the longitudinal profile shown in Figure 3. The sliding window is defined by the Galactic latitude range  $-1.5^\circ \leq l \leq +1.0^\circ$ , spans  $\Delta w = 15^\circ$  is Galactic longitude, with the windows being spaced  $\Delta s = 1^\circ$  apart (for a description of the chosen sliding window parameters, see [1]). Also shown is the large-scale  $\gamma$ -ray

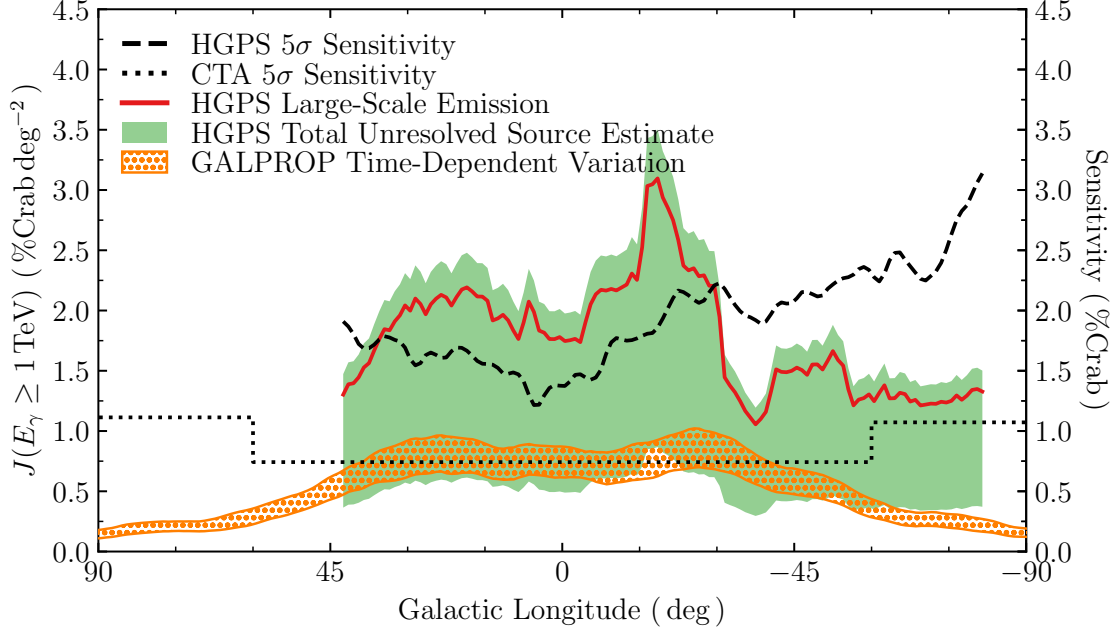


**Figure 3:** The longitudinal profile for the HGPS emission after catalogued sources are subtracted (see [1]) is shown in red. Accounting for the unresolved source contribution to the diffuse emission in the HGPS emission (see [1], and references therein) is shown by the green shaded band. The variation in the simulated GALPROP  $\gamma$ -ray spectra for a 5 Myr period is shown by the orange hatched band. All profiles are computed using a sliding window analysis (see [1], and references therein) for the integrated  $\gamma$ -ray emission for energies  $>1$  TeV, and are shown in units of  $\%Crab\ deg^{-2}$ . The  $5\sigma$  sensitivity for the HGPS is shown by the dashed black line and the sensitivity for the planned CTA GPS is shown by the dotted black line, with both sensitivities given in units of  $\%Crab$ .

emission from the HGPS [12] after subtracting the  $\gamma$ -ray emission from catalogued  $\gamma$ -ray sources. Estimates of the unresolved  $\gamma$ -ray source component to the large-scale emission observed in the HGPS vary between 13% to 60% (see [13, 14]). The longitudinal profile after accounting for the unresolved sources and after accounting for the flux uncertainty of the HGPS is shown in green. The residual emission found after accounting for both the catalogued and unresolved source components is an estimate of the large-scale diffuse emission in the TeV energy regime.

#### 4. Discussion

The electron flux at the Solar location is not representative of the Galactic CR flux. The local VHE CR electron population only probes the nearest  $\sim 100$ – $500$  pc region around the local environment. The local CR electron flux, and the break observed in the TeV energy regime, arises naturally from a population of discrete CR electron accelerators. Hence, the local CR electron spectrum, especially for energies above 100 GeV, can only be considered a snapshot in time. As there is an observed break in the local electron spectrum (as shown in Figure 1), there is likely no electron accelerator near the Solar location at the current time. As the break is a feature of the local

environment, no Galactic CR propagation code should normalise the Galactic CR electron density to the local flux above 100 GeV.

The energy of the electron spectral cut off, as well as the strength of the cut off, will depend on the electron injection spectrum. Currently, we considered only an average CR source class that injects both hadrons and leptons into the ISM. Considering the hadronic and leptonic sources separately may be necessary in future work and will likely increase the observed variation in the  $\gamma$ -ray fluxes.

To reproduce the observed cut off in the local electron spectrum it is becoming common to introduce a cut off to the electron injection spectrum around 10 TeV, suppressing IC emission in the TeV energy range. Given the large number of leptonic sources found by LHAASO, any potential break in the electron injection spectrum is likely to be found  $>100$  TeV. When using an electron cut off at  $\sim 10$  TeV, reproducing the  $\gamma$ -ray emission observed by LHAASO then requires boosting the hadronic emission by implicitly adding a collection of unresolved CR hadron accelerators with hard injection spectra. However, the modelled IC emission component shown in [Figure 2](#) adequately describes both the spectral shape and intensity of the LHAASO flux points. The IC emission found here can be considered as leptonic emission from an ensemble of unresolved CR electron accelerators.

For the  $>1$  TeV longitudinal profile ([Figure 3](#)), the variation found from injecting CRs from localised and randomly-placed CR sources is similar to the modelling uncertainty found across a grid of source distributions, ISRF models, and GMF models [1]. For further discussion on the GALPROP emission and the comparison to the HGPS, see [1]. The variation in the  $\gamma$ -ray emission predicted by GALPROP depends on the CR source parameters, particularly the source lifetime and source creation rate. These will be investigated further in future work.

## Acknowledgments

This research was supported by an Australian Government Research Training Program Scholarship, as well as student travel grants from both the Astronomical Society of Australia and the Australian Institute of Physics. GALPROP development is partially funded via NASA grants NNX17AB48G, 80NSSC22K0718, and 80NSSC22K0477. Some of the results in this poster have been derived using the HEALPix [7] and Astropy [15, 16] packages. This work was supported with supercomputing resources provided by the Phoenix HPC service at the University of Adelaide, and we want to thank Dr. F. Voisin in particular for his many hours spent configuring the HPC service to work efficiently with GALPROP.

## References

- [1] P.D. Marinos, G.P. Rowell, T.A. Porter and G. Jóhannesson, *The Steady-State Multi-TeV Diffuse Gamma-Ray Emission Predicted with GALPROP and Prospects for the Cherenkov Telescope Array*, *MNRAS* **518** (2023) 5036 [[2211.01619](#)].
- [2] T.A. Porter, G. Jóhannesson and I.V. Moskalenko, *Deciphering Residual Emissions: Time-dependent Models for the Nonthermal Interstellar Radiation from the Milky Way*, *ApJ* **887** (2019) 250 [[1909.02223](#)].

- [3] T.A. Porter, G. Jóhannesson and I.V. Moskalenko, *The GALPROP Cosmic-ray Propagation and Nonthermal Emissions Framework: Release v57*, *ApJS* **262** (2022) 30 [2112.12745].
- [4] A.W. Strong and I.V. Moskalenko, *Propagation of Cosmic-Ray Nucleons in the Galaxy*, *ApJ* **509** (1998) 212 [astro-ph/9807150].
- [5] I.V. Moskalenko and A.W. Strong, *Production and Propagation of Cosmic-Ray Positrons and Electrons*, *ApJ* **493** (1998) 694 [astro-ph/9710124].
- [6] G. Jóhannesson, T.A. Porter and I.V. Moskalenko, *The three-dimensional spatial distribution of interstellar gas in the milky way: Implications for cosmic rays and high-energy gamma-ray emissions*, *ApJ* **856** (2018) 45.
- [7] K.M. Górski, E. Hivon, A.J. Banday, B.D. Wandelt, F.K. Hansen, M. Reinecke et al., *HEALPix: A Framework for High-Resolution Discretization and Fast Analysis of Data Distributed on the Sphere*, *ApJ* **622** (2005) 759 [arXiv: astro-ph/0409513].
- [8] D. Kerszberg, *Etude du fond diffus galactique des électrons et positrons et étude des performances de la seconde phase de l'expérience H.E.S.S.*, Ph.D. thesis, LPNHE, 2017.
- [9] AMS COLLABORATION collaboration, *Electron and Positron Fluxes in Primary Cosmic Rays Measured with the Alpha Magnetic Spectrometer on the International Space Station*, *Phys. Rev. Lett.* **113** (2014) 121102.
- [10] DAMPE Collaboration, G. Ambrosi, Q. An, R. Asfandiyarov, P. Azzarello, P. Bernardini et al., *Direct detection of a break in the teraelectronvolt cosmic-ray spectrum of electrons and positrons*, *Nature* **552** (2017) 63 [1711.10981].
- [11] Z. Cao, F. Aharonian, Q. An, Axikegu, Y.X. Bai, Y.W. Bao et al., *Measurement of ultra-high-energy diffuse gamma-ray emission of the Galactic plane from 10 TeV to 1 PeV with LHAASO-KM2A*, *arXiv e-prints* (2023) arXiv:2305.05372 [2305.05372].
- [12] H. Abdalla, A. Abramowski, F. Aharonian, F. Ait Benkhali, E.O. Angüner, M. Arakawa et al., *The H.E.S.S. galactic plane survey*, *A&A* **612** (2018) A1.
- [13] C. Steppa and K. Egberts, *Modelling the galactic very-high-energy  $\gamma$ -ray source population*, *A&A* **643** (2020) A137.
- [14] M. Cataldo, G. Pagliaroli, V. Vecchiotti and F.L. Villante, *The tev gamma-ray luminosity of the milky way and the contribution of h.e.s.s. unresolved sources to very high energy diffuse emission*, *ApJ* **904** (2020) 85.
- [15] Astropy Collaboration, T.P. Robitaille, E.J. Tollerud, P. Greenfield, M. Droettboom, E. Bray et al., *Astropy: A community Python package for astronomy*, *A&A* **558** (2013) A33 [1307.6212].
- [16] Astropy Collaboration, A.M. Price-Whelan, B.M. Sipőcz, H.M. Günther, P.L. Lim, S.M. Crawford et al., *The Astropy Project: Building an Open-science Project and Status of the v2.0 Core Package*, *AJ* **156** (2018) 123 [1801.02634].